Article

Hydrogen and Deuterium Solubility in Commercial Pd–Ag Alloys for Hydrogen Purification

Annalisa Paolone [1],* , **Silvano Tosti** [2], **Alessia Santucci** [2], **Oriele Palumbo** [1] **and Francesco Trequattrini** [1,3]

1   Consiglio Nazionale delle Ricerche, Istituto dei Sistemi Complessi, U.O.S. La Sapienza, Piazzale A. Moro 5, 00185 Roma, Italy; oriele.palumbo@roma1.infn.it (O.P.); francesco.trequattrini@roma1.infn.it (F.T.)
2   Dipartimento Fusione e Tecnologie per la Sicurezza Nucleare, ENEA, Via E. Fermi 45, 00044 Frascati (RM), Italy; silvano.tosti@enea.it (S.T.); alessia.santucci@enea.it (A.S.)
3   Dipartimento di Fisica, Sapienza Università di Roma, Piazzale A. Moro 5, 00185 Roma, Italy
*   Correspondence: annalisa.paolone@roma1.infn.it; Tel.: +39-06-4991-4400

Abstract: Pd–Ag alloys with compositions close to 23–25% Ag are considered as a benchmark for hydrogen permeability. They are used in small scale reactors for hydrogen separation and purification. Permeability and solubility are strictly mathematically correlated, and the temperature dependence of solubility can provide useful information about the physical state of the material, the hydrogenation enthalpy, and the occurrence of different thermodynamic states. While the permeability of Pd–Ag alloys has been largely investigated, solubility measurements are available only in a restricted temperature range. In this paper, we extend solubility measurements up to 7 bar for $Pd_{77}Ag_{23}$ in the temperature range between 25 °C and 400 °C and for $Pd_{30}Ag_{70}$ for temperatures between 190 °C and 300 °C. The occurrence of solid solutions or hydride phases is discussed, and the hydrogenation enthalpy is calculated.

Keywords: hydrogen purification; hydrogen solubility; Sieverts measurements

1. Introduction

It has been reported that nearly 2% of the world's energy is stored in the hydrogen industrially produced each year. The major part of this hydrogen is used in chemical, petrochemical, metallurgical, pharmaceutical, and textile industries in order to manufacture a large number of products [1]. One of the main problems concerning hydrogen production [2–4] is its separation and purification from less desired gases by means of cost-effective processes. There are mainly three types of purification methods: (1) pressure swing adsorption (PSA), (2) fractional/cryogenic distillation, or (3) membrane separation [1]. PSA and distillation are in commercial operation, even though they are expensive and energy demanding. For small-scale applications and in order to achieve an ultra-high pure grade (>99.999%) of the released hydrogen, the membrane separation methods is currently believed to be the best choice, as it offers low energy consumption, possibility for continuous operation, lower investment costs, easy operation, and ultimately cost effectiveness [1].

The cheapest type of membranes for hydrogen separation are the polymeric ones that are already used in industrial processes, such as hydrogen separation in refineries and the petrochemical industry, the production of technical grade nitrogen, and the separation of CO_2 from CH_4 or N_2 [5–7]. However, the use of polymeric membranes is limited to temperatures below 100 °C and in applications in which the purity of the permeated gas is not a primary concern, as their selectivity is relatively low (not exceeding 100 [6]). Moreover, they suffer from swelling and poisoning [1]. Another concern about polymer membranes is the need to recover the toxic by-products for their production [7].

In general, when selectivity is important and higher temperatures are needed, the membrane separation techniques are based on permeators [8–10] in which hydrogen molecules are catalytically ionized to obtain H^+ ions on one of the surfaces of metallic membranes. The H^+ ions enter into the material and diffuse through the membrane towards the other surface, due to the gradient of pressure and concentration. After travelling along the whole membrane, finally H^+ ions can recombine on the second surface of the membrane to form ultrapure H_2 molecules. In general, a large variety of metallic alloys, both crystalline and amorphous [11,12], show high selectivity for hydrogen and this characteristic makes the ultrapure grade of the hydrogen gas permeated through the metallic membranes obtainable [1]. However, a proper choice of the metal should be made to ensure a large hydrogen diffusion coefficient in the metal [1,8,13]. One metal that displays a large diffusion coefficient is Pd [14]. For this metal, the adsorption and dissociation reactions, and the reverse ones, occurring on the surfaces of the membranes, are very fast. Therefore, the controlling mass transfer mechanism is the diffusion of hydrogen through the metal lattice. Accordingly, the hydrogen permeation flux through a dense metal wall is well described by the equation:

$$J = \frac{Pe}{t}\left(p_{up}^{0.5} - p_{down}^{0.5}\right) \tag{1}$$

where J is the hydrogen permeation flux (mol·m^{-2} s^{-1}), p_{up} and p_{down} (Pa) are the hydrogen partial pressures in the upstream and in the downstream side, respectively, t (m) is the membrane thickness, and Pe (mol·m^{-1}·s^{-1}·Pa$^{-0.5}$) is the hydrogen permeability. It is well known that the permeability coefficient is given by the product:

$$Pe = D \times S \tag{2}$$

where D is the diffusion coefficient (m^2 s^{-1}), and S the solubility coefficient (mol m^{-3} Pa$^{-0.5}$). As a consequence of the above considerations, the metals suitable for the hydrogen separation have to exhibit high hydrogen permeability (i.e., an optimum combination of hydrogen solubility and diffusivity) and low surface resistance.

One of the most important drawbacks of Pd is that, when subjected to repeated hydrogenation/dehydrogenation cycles under specific operative conditions, it can suffer from embrittlement due to the mismatch between the lattice parameter of the α, solid solution, and β, hydride, phases. Alloying with other metals has been recognized as a method that mitigates such an inconvenience, and Pd–Ag alloys in particular have been largely investigated. Among Pd–Ag alloys, the best compromise between the mitigation of lattice mismatch, the hydrogen diffusion coefficient, and permeability is obtained around the composition $Pd_{77}Ag_{23}$ or $Pd_{75}Ag_{25}$ [15], while the alloy $Pd_{30}Ag_{70}$ is commercially available for high temperature brazing and is used for joining the Pd–Ag permeator tubes to the stainless steel modules. Furthermore, the alloying with Ag increases the mechanical strength of pure Pd, thus improving the efficiency and reliability of the membrane modules.

Many studies about bulk Pd-membranes are devoted to the investigation of the permeability as a function of temperature [16–20], which is the physical quantity of principal interest for applications. Less attention has been devoted to the solubility of hydrogen in Pd–Ag alloys, which however gives important information about the physical state of the alloys. Therefore, in order to fill this gap, we measured the solubility of hydrogen in two commercially available alloys, $Pd_{77}Ag_{23}$ and $Pd_{30}Ag_{70}$. We extended solubility investigation in the pressure ($p < 7$ bar) and temperature (T < 400 °C) ranges usually exploited for permeation measurements and for applications in permeators made of thin-walled tubes.

2. Materials and Methods

A $Pd_{77}Ag_{23}$ (wt %) foil with a thickness of 25 μm was purchased from Goodfellow, while a $Pd_{30}Ag_{70}$ (wt %) foil 150 μm thick was obtained from Johnson Matthey.

Small pieces of the membranes (with typical dimensions of ~20 mm × 7 mm) were cut and used for measurements of pressure–composition curves in a homemade Sieverts apparatus [21,22] working up to a 200 bar pressure and a 500 °C temperature. The amount of hydrogen exchanged between the gas atmosphere and the solid samples was measured by the pressure variation in calibrated cylinders connected by Swagelok tubes to the reaction chamber, where the sample was placed. The data acquisition was performed by means of a homemade computer program developed in the Labview language. Practically, the time evolution of the pressure detected by two micro-Baratron transducers working between 0 and 7 bar and between 0 and 200 bar, respectively, of the temperature of the five cylinders, and of the tubes connecting the cylinders and the reaction chamber was recorded. The real gas state equation was used to calculate the exchanged hydrogen moles. The hydrogenation procedure was extended until a steady state was obtained and no more hydrogen was absorbed by the membranes. A total mass of ~148 mg and ~906 mg were used for $Pd_{77}Ag_{23}$ and $Pd_{30}Ag_{70}$, respectively. Experiments were conducted at temperatures between 25 and 400 °C for $Pd_{77}Ag_{23}$ and between 190 and 300 °C for $Pd_{30}Ag_{70}$. For both samples, the maximum applied pressure is ~7 bar. In order to perform such gas sorption measurements, hydrogen (purity: ≥99.9999%) and deuterium (purity: ≥99%) were purchased from Società Italiana Acetilene e Derivati (Rome, Italy).

3. Results and Discussion

A surface analysis of the $Pd_{77}Ag_{23}$ and $Pd_{30}Ag_{70}$ samples was performed by means of a SEM/EDX technique to investigate the alloy composition and the absence of impurities and defects. Micrographs Figure 1a,b show the $Pd_{77}Ag_{23}$ sample, while Figure 1c,d refer to the $Pd_{30}Ag_{70}$ sample. The surface of the $Pd_{77}Ag_{23}$ sample is rather smooth and regular, with only few irregularities mainly due to the manufacture procedure (i.e., lamination); in the $Pd_{30}Ag_{70}$ sample, the effects of the lamination process are much more evident. For this reason, SEM analysis was also performed along the cross-section. As shown in Figure 2, SEM analysis revealed that the scratches due to the lamination involve only the surface of the sample and not the bulk of the materials, which appears rather regular and homogeneous.
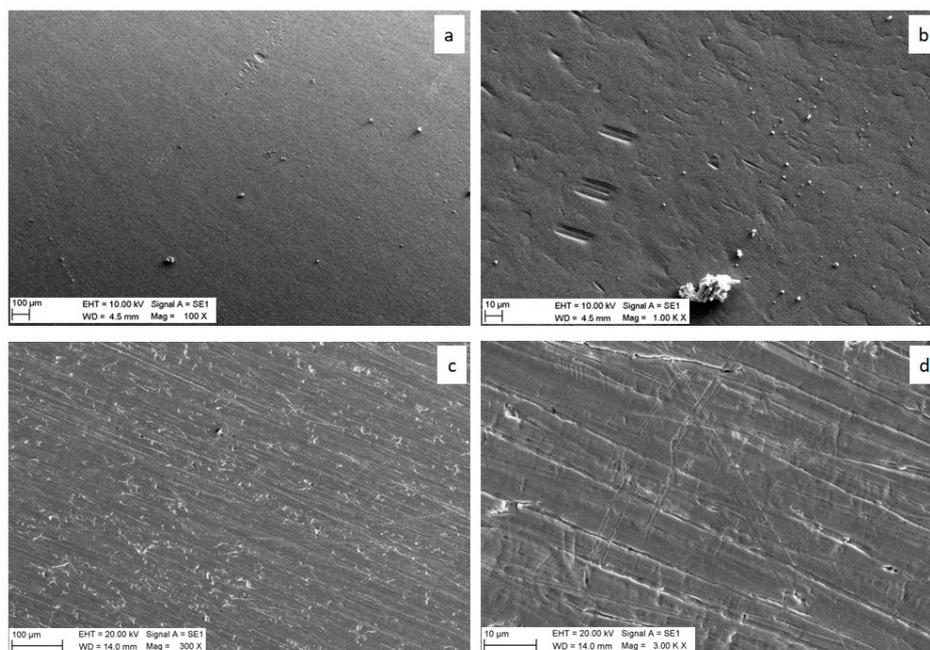

Figure 1. SEM micrographs of the two samples at different magnitude: (**a**,**b**) refer to the $Pd_{77}Ag_{23}$ sample, while (**c**,**d**) regard the $Pd_{30}Ag_{70}$ sample.
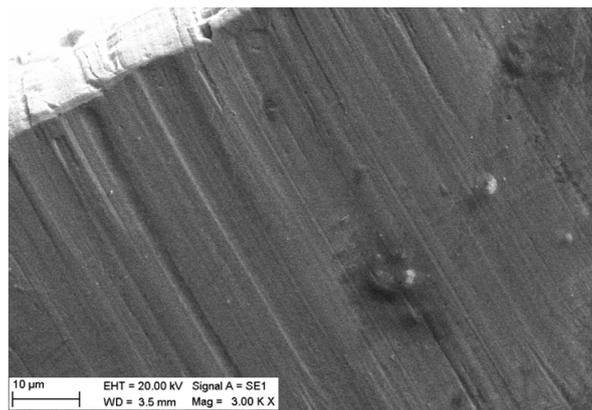
Figure 2. SEM micrographs of the cross section of the $Pd_{30}Ag_{70}$ sample.

Regarding the composition and the presence of impurities, in the $Pd_{77}Ag_{23}$ sample EDX has detected a composition of 78 atom % of Pd and 22 atom % of Ag, while in the $Pd_{30}Ag_{70}$ sample the measured composition is 31 atom % of Pd and 69 atom % of Ag. No other elements, besides some organic compounds on the surface, have been observed.

The solubility measurements are reported in Figure 3 for both samples, in the form of pressure-composition isotherms. The hydrogen concentration is expressed as H/M, i.e., the number of hydrogen atoms per atom of metal [23]. The error bars on the single measurements are smaller than the symbols. Moreover, reproducibility was checked by duplicate measurements at selected temperatures.
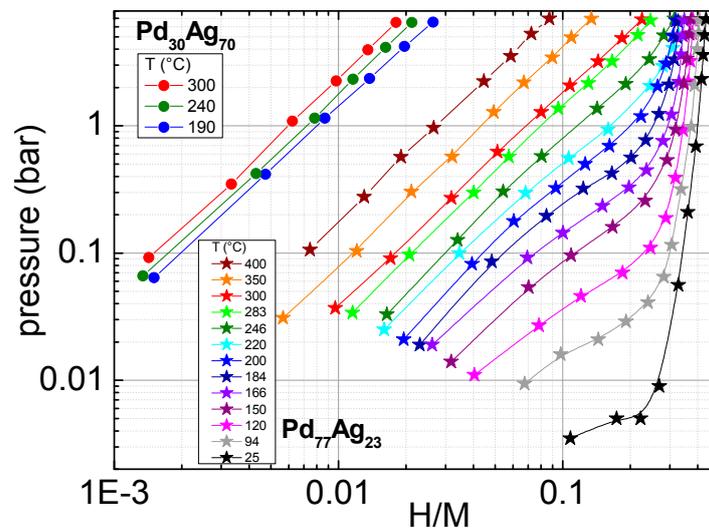

Figure 3. Absorption pressure–composition isotherms measured at selected temperatures for $Pd_{77}Ag_{23}$ and $Pd_{30}Ag_{70}$.

The solubility increases for both samples as temperature decreases. Moreover, at selected temperature and pressure conditions, the hydrogen concentration in $Pd_{77}Ag_{23}$ is at least one order of magnitude higher than in $Pd_{30}Ag_{70}$. In Figure 3, one can observe different shapes of the sorption curves as a function of the absorption temperature and Ag content. In fact, $Pd_{30}Ag_{70}$ shows at all the three temperatures (above 190 °C) a linear dependence of $\ln(p)$ from $\ln(c)$. This behavior is expected when a single phase is present in the sample. As the hydrogen concentration is extremely low (lower than 10^{-2}), the phase should be the α one, i.e., the solid solution of hydrogen in the metal matrix. This fact is in agreement with previous investigation of the Pd–Ag–H phase diagram in which, for concentration higher than 30% of Ag, only the α phase seems to occur [24,25]. In the case of $Pd_{77}Ag_{23}$ the high temperature curves ($T > 280$ °C) clearly

display a similar linear dependence, witnessing the occurrence of only the α phase. At lower temperatures, especially below 200 °C, two inflections centered around H/M ~0.08 and 0.25 are visible. This behavior suggests the occurrence of a solid solution at low concentrations and the gradual transformation from the α to the β hydride phase at higher concentrations. This findings are in close agreement with the existence of a critical temperature reported between 283 and 295 °C for Pd–H system [26]: above such a temperature only solid solution of H in palladium can be observed, while at lower temperatures, a transition toward the hydride phase has been reported.

To the best of our knowledge, the p-c curves of $Pd_{30}Ag_{70}$ had never been investigated before, while some previous investigations of $Pd_{77}Ag_{23}$ or $Pd_{75}Ag_{25}$ are available in more restricted temperature ranges, mainly below the critical temperature [16,27,28]. The $Pd_{75}Ag_{25}$ sample investigated by Ross et al. was not commercial and was displayed a lower maximum capacity of hydrogen storage, while the value of the pressure plateau displayed by the same authors up to temperatures below 250 °C seems to be comparable to those here reported [16]. Additionally, the samples studied by Flanagan et al. showed a lower maximum hydrogen capacity [27]. The measurements reported by Anand et al. on $Pd_{77}Ag_{23}$ extended only up to 150 °C on a sample prepared by arc melting [28].

A general consideration about the kinetics of absorption in the two membranes (results not shown): while the kinetics of $Pd_{77}Ag_{23}$ is extremely fast (full hydrogen absorption in less than 150 s at 300 °C), the time dependence of the hydrogen solubility in $Pd_{30}Ag_{70}$ is extremely slow, even at high temperatures (full hydrogen absorption in ~3000 s at 300 °C) (see Figure S1).

From the pressure-composition isotherms, the hydrogenation enthalpy can be calculated by means of the so-called van't Hoff plot, reporting the logarithm of the equilibrium pressure versus the inverse of the temperature. For materials exhibiting flat pressure plateau centered at p^*, the van't Hoff plot reports $\ln(p^*)$ vs. $1/T$, and the slope of the best fit lines provides the hydrogenation enthalpy, ΔH_{hyd}. In materials showing no pressure plateau, one can still construct a van't Hoff plot reporting $\ln(p)$ vs. $1/T$, where p is the pressure at a fixed value of H/M at the various temperatures. Additionally, in this case, one can estimate the hydrogenation enthalpy, ΔH_{hyd}, from the slope of the plot [29,30]. In order to construct such a graph, the experimental pressure–composition isotherms were interpolated by means of beta splines, thanks to a program based on the Labview (National Instruments, Austin, TX, USA) routines.

Figures 4 and 5 display the van't Hoff plot of $Pd_{77}Ag_{23}$ in the two different zones of the pressure–composition graph: low c and high T (i.e., in the α phase), higher c, low T (i.e., in the coexistence region of the α and the β phase).
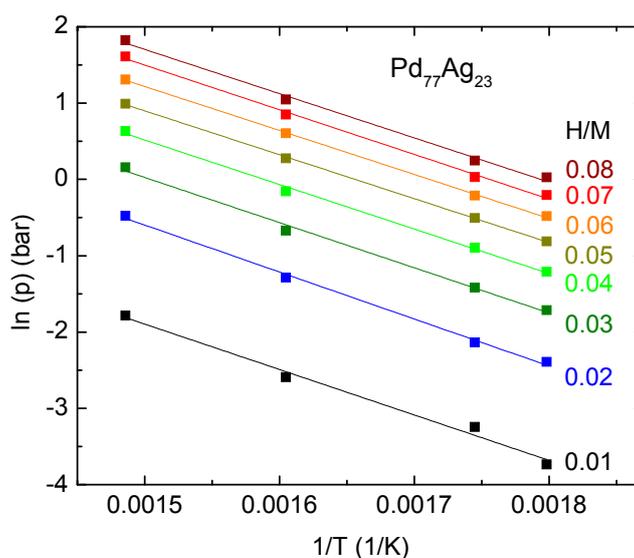

Figure 4. Van't Hoff plot for $Pd_{77}Ag_{23}$ at a fixed H/M (the number of hydrogen atoms per atom of metal) in the low concentration region and best fit lines to calculate the hydrogenation enthalpy.
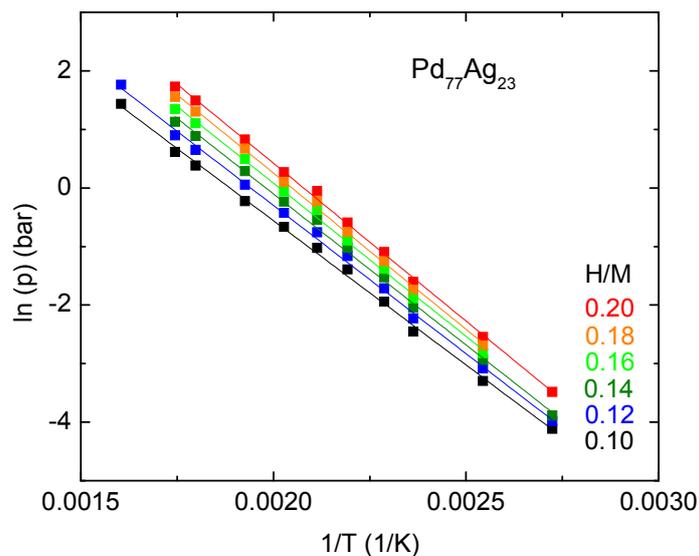
Figure 5. Van't Hoff plot for $Pd_{77}Ag_{23}$ at a fixed H/M in the higher concentration region and best fit lines to calculate the hydrogenation enthalpy.

The hydrogenation enthalpy values obtained in the two regions are 49 ± 2 kJ/mol for low c and high T and 43 ± 2 kJ/mol for low temperatures and higher concentrations. This values are quite in good agreement with values obtained by calorimetric and volumetric techniques in Pd–H (~38 kJ/mol) [24] and with the value for the α to the β phase transition reported by Anand et al. for $Pd_{77}Ag_{23}$ below 150 °C (42.2 ± 0.5 kJ/mol) [28].

The van't Hoff plot for $Pd_{30}Ag_{70}$ is reported in Figure 6. The best fit provides a value of ΔH_{hyd} of ~10.8 ± 0.6 kJ/mol, a value much lower than in the case of $Pd_{77}Ag_{23}$. Indeed, previous investigation of the $Pd_{100-x}Ag_xH$ system by calorimetric measurements indicated that the absolute value of the hydrogenation enthalpy has a maximum value for x of ~40 and decreases on the further increase of the silver content in the alloys up to an x value of ~50. No additional information about the hydrogenation enthalpy of the $Pd_{100-x}Ag_xH$ system are available for higher x values [27].
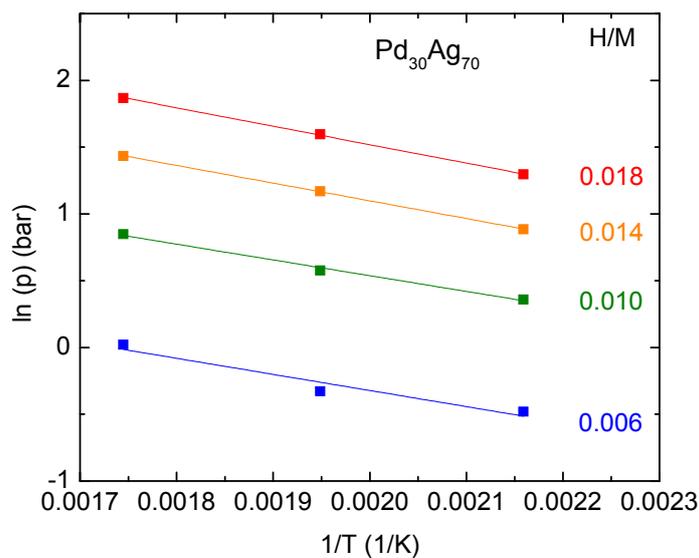

Figure 6. Van't Hoff plot for $Pd_{30}Ag_{70}$ at a fixed H/M in the whole concentration region and best fit lines.

Finally, we investigated the isotopic effect between hydrogenation and deuteration for $Pd_{77}Ag_{23}$ at 94 °C, as no information is available for such a content of Ag in the Pd–Ag membranes. Due to the limitations of our inlet line for deuterium, we extended our measurements only up to 2 bar, so we chose a low temperature in order to study the whole absorption curve. The two absorption isotherms measured for hydrogenation and deuteration are reported in Figure 7. Above a c value of ~0.3 H/M, the two curves coincide, while for lower hydrogen concentrations, the D absorption curves is displaced towards higher pressures by almost one order of magnitude. It is well known, indeed, that palladium has an unusual isotopic effect: in normal compounds, the curves corresponding to deuteration are displaced toward lower pressure, while in the case of palladium, the opposite effect occurs. Similar behavior, with a higher pressure plateau for deuterated samples, has already been reported by Anand et al. for $Pd_{75}Ag_{25}$ [28] and by Hara et al. for $Pd_{93}Ag_7$ [31].
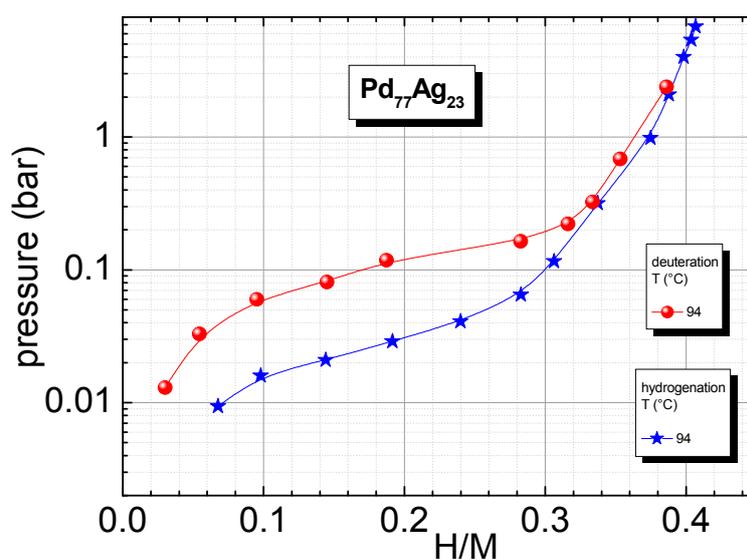

Figure 7. Comparison of the pressure-composition isotherm of $Pd_{77}Ag_{23}$ at 94 °C for hydrogen and deuterium absorption.

4. Conclusions

In this paper, an extensive study of the solubility of hydrogen in two commercial Pd–Ag alloys up to p = 7 bar is reported. For $Pd_{77}Ag_{23}$ ($Pd_{30}Ag_{70}$), the investigated temperature range extends from 25 °C up to 400 °C (190 °C–300 °C), well above the temperature range investigated in the previous literature for compositions close to $Pd_{77}Ag_{23}$. Below ~280 °C, $Pd_{77}Ag_{23}$ displays the existence of the β phase, with a hydrogenation enthalpy of 43 ± 2 kJ/mol. Above such a temperature, only a solid solution phase is observed, and the calculated ΔH_{hyd} is ~49 ± 2 kJ/mol. The study was extended to a much higher Ag concentration in the Pd–Ag alloy, i.e., to $Pd_{30}Ag_{70}$, a composition never investigated before. $Pd_{30}Ag_{70}$ shows the existence of an α phase in the whole temperature range, with a lower hydrogenation enthalpy (~10.8 ± 0.6 kJ/mol), and a maximum solubility one order of magnitude lower than that of $Pd_{77}Ag_{23}$. Moreover, the hydrogenation kinetics of $Pd_{77}Ag_{23}$ is slower than that of $Pd_{30}Ag_{70}$ by one order of magnitude.

Author Contributions: Annalisa Paolone, Alessia Santucci, and Silvano Tosti conceived the experiments; Alessia Santucci and Silvano Tosti performed the SEM/EDX measurements and analysis; Annalisa Paolone, Oriele Palumbo, and Francesco Trequattrini performed the Sieverts measurements; Annalisa Paolone analyzed the Sieverts data and wrote the paper. All authors discussed the data and made the same conclusions.

Conflicts of Interest: The authors declare no conflict of interest.

References

1. Ockwig, N.W.; Nenoff, T.M. Membranes for Hydrogen Separation. *Chem. Rev.* **2007**, *107*, 4078–4110. [CrossRef] [PubMed]
2. Orhan, M.F.; Dincer, I.; Rosen, M.A.; Kanoglu, M. Integrated hydrogen production options based on renewable and nuclear energy sources. *Renew. Sustain. Energy Rev.* **2012**, *16*, 6059–6082. [CrossRef]
3. Biccikovci, O.; Straka, P. Production of hydrogen from renewable resources and its effectiveness. *Int. J. Hydrog. Energy* **2012**, *37*, 11563–11578. [CrossRef]
4. Nowotny, J.; Veziroglu, T.N. Impact of hydrogen on the environment. *Int. J. Hydrog. Energy* **2011**, *36*, 13218–13224. [CrossRef]
5. Budd, P.M.; McKeown, N.B. Highly permeable polymers for gas separation membranes. *Polym. Chem.* **2010**, *1*, 63–68. [CrossRef]
6. Yampolskii, Y. Polymer Gas Separation Membranes. *Macromolecules* **2012**, *45*, 3298–3311. [CrossRef]
7. Razali, M.; Kim, J.F.; Attfield, M.; Budd, P.M.; Drioli, E.; Lee, Y.M.; Szekely, G. Sustainable wastewater treatment and recycling in membrane manufacturing. *Green Chem.* **2015**, *17*, 5196–5205. [CrossRef]
8. Gallucci, F.; Medrano, J.A.; Fernandez, E.; Melendez, J.; van Sint Annaland, M.; Pacheco-Tanaka, D.A. Advances on High Temperature Pd-Based Membranes and Membrane Reactors for Hydrogen Purification and Production. *J. Membr. Sci. Res.* **2017**, *3*, 142–156. [CrossRef]
9. Tosti, S. Pd-Based Membranes and Membrane Reactors for Hydrogen Production. In *Membrane Fabrication*; Hilal, N., Ismail, A.F., Wright, C.J., Eds.; CRC Press: Boca Raton, FL, USA, 2015; Chapter 13, ISBN 978-1-4822-1045-3.
10. Yun, S.; Oyama, S.T. Correlations in palladium membranes for hydrogen separation: A review. *J. Membr. Sci.* **2011**, *375*, 28–45. [CrossRef]
11. Sarker, S.; Chandra, D.; Hirscher, M.; Dolan, M.; Isheim, D.; Wermer, J.; Viano, D.; Baricco, M.; Udovic, T.J.; Grant, D.; et al. Developments in the Ni–Nb–Zr Amorphous Alloy Membranes. *Appl. Phys. A* **2016**, *122*, 168. [CrossRef]
12. Santucci, A.; Tosti, S.; Basile, A. Alternatives to palladium in membranes for hydrogen separation: Nickel, niobium and vanadium alloys, ceramic supports for metal alloys and porous glass membranes. In *Handbook of Membrane Reactors*; Basile, A., Ed.; Woodhead Publishing Series in Energy: Cornwall, UK, 2013; Volume 1, Chapter 4, pp. 183–217, ISBN 978-0-85709-414-8.
13. Conde, J.J.; Maroño, M.; Sánchez-Hervás, J.M. Pd-Based Membranes for Hydrogen Separation: Review of Alloying Elements and Their Influence on Membrane Properties. *Sep. Purif. Rev.* **2017**, *46*, 152–177. [CrossRef]
14. Steward, S.A. Review of Hydrogen Isotope Permeability through Metals. In *U.S. National Laboratory Report*; UCRL-53441; Lawrence Livermore National Lab.: Livermore, CA, USA, 1983.
15. Tosti, S. Membranes and Membrane Reactors for tritium Separation. In *Tritium in Fusion: Production, Uses and Environmental Impact*; Tosti, S., Ghirelli, N., Eds.; Nova Science Publishers: Hauppauge, NY, USA, 2013; Chapter 6, pp. 203–240, ISBN 978-1-62417-270-0.
16. Serra, E.; Kemali, M.; Perujo, A.; Ross, D.K. Hydrogen and deuterium in Pd-25 Pct Ag alloy: Permeation, diffusion, solubilization, and surface reaction. *Metall. Mater. Trans. A* **1998**, *29*, 1023–1028. [CrossRef]
17. Okazaki, J.; Pacheco Tanaka, D.A.; Llosa Tanco, M.A.; Wakui, Y.; Mizukami, F.; Suzuki, T.M. Hydrogen permeability study of the thin Pd–Ag alloy membranes in the temperature range across the α-β phase transition. *J. Membr. Sci.* **2006**, *282*, 370–374. [CrossRef]
18. Wang, D.; Flanagan, T.B.; Shanahan, K. Diffusion of H through Pd-Ag Alloys (423–523 K). *J. Phys. Chem. B* **2008**, *112*, 1135–1148. [CrossRef] [PubMed]
19. Zhang, K.; Gade, S.K.; Hatlevik, Ø.; Way, J.D. A sorption rate hypothesis for the increase in H_2 permeability of palladium-silver (Pd–Ag) membranes caused by air oxidation. *Int. J. Hydrog. Energy* **2012**, *37*, 583–593. [CrossRef]
20. Suzuki, A.; Yukawa, H.; Nambu, T.; Matsumoto, Y.; Murata, Y. Anomalous Temperature Dependence of Hydrogen Permeability through Palladium-Silver Binary Alloy Membrane and Its Analysis Based on Hydrogen Chemical Potential. *Mater. Trans.* **2016**, *57*, 695–702. [CrossRef]

21. Palumbo, O.; Brutti, S.; Trequattrini, F.; Sarker, S.; Dolan, M.; Chandra, D.; Paolone, A. Temperature dependence of the Elastic Modulus of $(Ni_{0.6}Nb_{0.4})_{1-x}Zr_x$ Membranes: Effects of Thermal Treatments and Hydrogenation. *Energies* **2015**, *8*, 3944–3954. [CrossRef]

22. Palumbo, O.; Trequattrini, F.; Vitucci, F.M.; Bianchin, A.; Paolone, A. Study of the hydrogenation /dehydrogenation process in the Mg-Ni-C-Al system. *J. Alloys Compd.* **2015**, *645*, S239–S241. [CrossRef]

23. Palumbo, O.; Trequattrini, F.; Sarker, S.; Hulyakar, M.; Pal, N.; Chandra, D.; Dolan, M.; Paolone, A. New Studies of the Physical Properties of Metallic Amorphous Membranes for Hydrogen Purification. *Challenges* **2017**, *8*, 4. [CrossRef]

24. Carson, A.W.; Lewis, F.A. Pressure-composition isotherms for the Pd+Ag+H system. *Trans. Faraday Soc.* **1967**, *63*, 1453–1457. [CrossRef]

25. Shu, J.; Granjean, B.P.A.; van Neste, A.; Kaliaguine, S. Catalytic Palladium-based Membrane Reactors: A Review. *Can. J. Chem. Eng.* **1991**, *69*, 1036–1060. [CrossRef]

26. Manchester, F.D.; San Martin, A.; Pitre, J.M. The H-Pd (hydrogen-palladium) system. *J. Phase Equil.* **1994**, *15*, 62–83. [CrossRef]

27. Flanagan, T.B.; Wang, D.; Luo, S. Thermodynamics of H in disordered Pd–Ag alloys from calorimetric and equilibrium pressure–composition-temperature measurements. *J. Phys. Chem. B* **2007**, *111*, 10723–10735. [CrossRef] [PubMed]

28. Anand, N.S.; Pati, S.; Avtar Jat, R.; Parida, S.C.; Mukerjee, S.K. Thermodynamics and kinetics of hydrogen/deuterium absorption and desorption in $Pd_{0.77}Ag_{0.23}$ alloy. *Int. J. Hydrog. Energy* **2015**, *40*, 444–450. [CrossRef]

29. Karger, B.L.; Snyder, L.R.; Horvath, C. *An Introduction to Separation Science*; Wiley: New York, NY, USA, 1973.

30. Palumbo, O.; Trequattrini, F.; Pal, N.; Hulyalkar, M.; Sarker, S.; Chandra, D.; Flanagan, T.; Dolan, M.; Paolone, A. Hydrogen absorption properties of amorphous $(Ni_{0.6}Nb_{0.4-y}Ta_y)_{100-x}Zr_x$ membranes. *Prog. Nat. Sci.* **2017**, *27*, 126–131. [CrossRef]

31. Hara, M.; Sakurai, J.; Akamaru, S.; Hashizume, K.; Nishimura, K.; Mori, K.; Okabe, T.; Watanabe, K.; Matsuyama, M. Thermodynamic and Magnetic Properties of $Pd_{0.93}Ag_{0.07}$ Hydride. *Mater. Trans.* **2007**, *48*, 3154–3159. [CrossRef]